Eur. Phys. J. Spec. Top.
https://doi.org/10.1140/epjs/s11734-024-01228-w

THE EUROPEAN PHYSICAL JOURNAL SPECIAL TOPICS

Regular Article

Stochastic nonlinear model for nanoparticles and viruses escape from endosomes

Vladimir Sholokhov[1,a], Eugenya V. Makoveeva[1,b], Sergei Fedotov[2,c], and Dmitri V. Alexandrov[1,d]

[1] Laboratory of Stochastic Transport of Nanoparticles in Living Systems, Laboratory of Multi-Scale Mathematical Modeling, Department of Theoretical and Mathematical Physics, Ural Federal University, Lenin ave., 51, Ekaterinburg 620000, Russian Federation
[2] Department of Mathematics, The University of Manchester, Manchester M13 9PL, UK

Received 23 March 2024 / Accepted 19 June 2024

Abstract A stochastic nonlinear model for Rab5 and Rab7 proteins describing the transformation of early endosomes into late endosomes was formulated. This model consists of two stochastic nonlinear differential equations for Rab5 and Rab7 protein levels on the endosome surface. The primary goal of this paper is to understand the impact of multiplicative noise on the nonlinear dynamics of Rab5 and Rab7. The main idea is to introduce the stochastic variable T, which defines the random time when the conversion from Rab5 to Rab7 occurs. It follows from the dynamics of pH level that T can also be considered as the escape time of pH-sensitive nanoparticles and viruses from endosomes. The probability density function for T was obtained numerically. It was shown that the average conversion time T is shifted to the right when compared to the deterministic one, potentially influencing the pH distribution function and, consequently, the average escape time of viruses and nanoparticles.

1 Introduction

The internalization of nanoparticles or viruses into the living cell occurs through receptor-dependent endocytosis involving the fusion of the nanoparticle/virus with the cell membrane [1, 2]. Understanding of this process is essential for the safe and efficient application of nanoparticles in medicine [3–5]. During capturing and absorbing the virus or nanoparticle, an intracellular vacuole (endosome) is generated, and subsequently, the endosome provides the transportation of nanoparticles and viruses along microtubules inside living cells [6, 7]. To avoid lysosomal degradation, the nanoparticles or viruses must exit the endosome and enter the cell cytoplasm. This occurs when the endosome acidifies and its pH drops [8–10]. Consequently, the stochastic residence time of pH-sensitive nanoparticles or viruses within endosomes is influenced by the ongoing endosomal acidification. The cytoplasmic pH is known to be close to 7.0, which decreases to about pH 6.4 in early endosomes and then to about pH 5.0 in lysosomes. The maturation of early endosomes into late endosomes is regulated by the conversion of Rab5 to Rab7 accompanied by concurrent acidification [11, 12]. It has been found that nanoparticles sensitive to pH conditions demonstrate an efficient ability to escape endosomes before the degradations in lysosomes. This explains the potential for these pH-sensitive nanoparticles to enhance targeted drug delivery and therapeutic applications [13–16].

Recently, a stochastic model for the dynamic behavior of active Rab5 and Rab7 proteins on endosome surfaces along with the acidification process determining the endosomal escape of pH-responsive nanoparticles and viruses has been developed [20, 21]. The authors employed a cutoff switch model [18] for the conversion of Rab5 to Rab7, used a linear version [19] and incorporated additive and multiplicative noises. By numerical simulations, they determined the marginal probability density for endosomal pH and computed the probability of the endosomal

[a] e-mail: vladimir.sholokhov@urfu.ru
[b] e-mail: e.v.makoveeva@urfu.ru
[c] e-mail: sergei.fedotov@manchester.ac.uk (corresponding author)
[d] e-mail: dmitri.alexandrov@urfu.ru

Published online: 03 July 2024

pH falling below a critical threshold. It gives the percentage of viruses and pH-responsive nanoparticles that successfully escape endosomes.

In this paper, we extend our previous analysis to include the nonlinear Rab5 to Rab7 conversion process. According to the nonlinear cutoff switch model [18], Rab5 triggers the activation of Rab7 until the level of Rab7 reaches a certain threshold, at which point in time it rapidly deactivates Rab5. This time T can be referred to as the conversion time. It represents a significant characteristic of this nonlinear cutoff switch model that finds strong support in the experimental data [18]. It follows from the dynamics of pH level that T can also be considered as the escape time of pH-sensitive nanoparticles and viruses from endosomes. The main objectives of this paper are to understand how multiplicative noise affects the nonlinear dynamics of Rab5 and Rab7. In particular, one of the aims is to find the probability distribution for T. From a mathematical point of view, we look at the conversion of Rab5 to Rab7 as a stochastic process that is a critical process in the regulation of trafficking the endosomes inside cells.

2 Nonlinear deterministic model for Rab5 and Rab7

The transition from early to late endosomes is controlled by the depletion of Rab5 protein on the surface of endosomes and the simultaneous increase of Rab7, a process known as Rab conversion [18]. In this section, we suggest the nonlinear model for Rab conversion involving only two variables $R_5(\tau)$ and $R_7(\tau)$ for active Rab5 and Rab7 proteins:

$$\frac{dR_5}{d\tau} = \nu_{50}N_s - f_5(R_5,\, R_7)R_7 - \nu_{55}R_5, \qquad \frac{dR_7}{d\tau} = f_7(R_5,\, R_7)R_5 - \nu_{77}R_7, \tag{1}$$

where τ is the time variable and nonlinear rate functions f_5 and f_7 are as follows:

$$f_5(R_5,\, R_7) = \frac{\nu_{57}R_5^3}{1 + e^{c_5(1-R_7)}}, \quad f_7(R_5,\, R_7) = \frac{\nu_{75}R_5}{1 + e^{c_7(0.93-R_7)^2}}. \tag{2}$$

The main idea of the dynamical system (1) and (2) is that Rab5 triggers the activation of Rab7, but Rab7 exhibits auto-activation while simultaneously suppressing Rab5. The rate of the activation of Rab5, which depends on the number of endosomes in the cell N_s, is described by the constant $\nu_{50}N_s$. The deterministic rate of gradual activation of Rab7 by Rab5 is given by constant ν_{75}, while constant ν_{57} characterizes the deterministic rate of inactivation of Rab5 by Rab7; the rate of self-inactivation for Rab5 and Rab7 is described by constants ν_{55} and ν_{77}. Two parameters in (2) c_5 and c_7 are constant. The nonlinear rate functions (2) are chosen to qualitatively match experimental data on the temporal evolution of Rab5 and Rab7 proteins [18].

The main difference between the linear and nonlinear models for Rab5 and Rab7 lies in the temporal dynamics. In the linear model [19–21], the dynamics of Rab5 and Rab7 exhibit relative smoothness. In the nonlinear model (1) and (2), the Rab5 protein decreases steadily until it undergoes a sudden drop during the conversion event. Figure 1 illustrates this rapid transition.

Unlike the linear system, nonlinear equations have a slower initial rate of growth for the variable Rab7. One can see from Fig. 1 that a rapid growth of Rab7 happens around time $T = 850$ s after which Rab7 approaches its steady-state value, whereas Rab5 experiences an initial increase to its peak value followed by a swift decline from $T = 850$ s to its steady-state value (see Fig. 1). This behavior of Rab5 and Rab7 is in good agreement with experimental data [18]. The variable T can be considered as the transition time from early endosomes to late

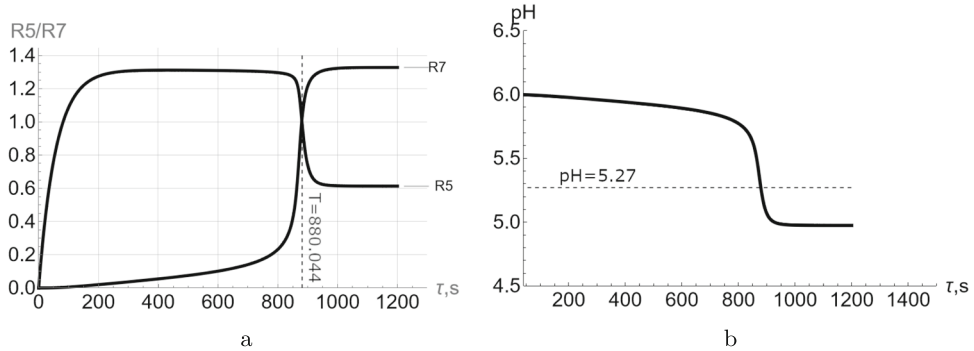

Fig. 1 Dynamics of protein levels Rab5 and Rab7, and pH level in the endosome obtained by numerical solutions of Eqs. (1) and (2). The values of parameters used for numerical simulations are listed in Table 1

Table 1 The values of the parameters from Eqs. (1) and (2) used for numerical simulations

Parameter	Value	Parameter	Value
c_5	5	ν_{57}	0.006 (s^{-1})
c_7	7	ν_{77}	0.0032 (s^{-1})
ν_{50}	$1.2 \cdot 10^{-5}$ (s^{-1})	ν_{75}	0.0045 (s^{-1})
$\nu_{50} N_s$	0.0045 (s^{-1})	ν_{55}	0.0175 (s^{-1})
p_H^l	4.5	p_H^e	6
τ_H	0.01 (s)		

endosomes, and it stands as a crucial parameter of the system (1) and (2). In the next section, we add multiplicative noises into the system (1) and (2) and analyze their impact on the distribution of the random conversion time T. It follows from the dynamics of pH level in Fig. 1 that T can also be considered as the escape time of pH-sensitive nanoparticles and viruses from endosomes.

3 Stochastic nonlinear model for Rab5 and Rab7

This section aims to examine the impact of multiplicative noise on the nonlinear model (1) and (2). In particular, we are interested in the distribution of the random transition time T from early endosomes to late endosomes. We write out the system of stochastic differential equations (SDE) for Rab5 and Rab7 in the following form:

$$\begin{aligned} dR_5(\tau) &= \nu_{50} N_s d\tau - \nu_{55} R_5(\tau) d\tau - f_5(R_5, R_7) R_7(\tau) d\tau + \sigma_5 f_5(R_5, R_7) R_7(\tau) dW_5, \\ dR_7(\tau) &= -\nu_{77} R_7(\tau) d\tau + f_7(R_5, R_7) R_5(\tau) d\tau + \sigma_7 f_7(R_5, R_7) R_5(\tau) dW_7, \end{aligned} \tag{3}$$

where σ_5 and σ_7 describe the strength of the multiplicative noises, $W_5(\tau)$ and $W_7(\tau)$ are independent Wiener processes.

The relaxation equation for endosomal pH can be written in the form

$$\frac{dp_H(\tau)}{d\tau} = -\frac{p_H(\tau) - p_H^s(R_5, R_7)}{\tau_H}, \tag{4}$$

where $p_H^s(R_5, R_7)$ is the steady endosomal pH, and τ_H is the relaxation constant. $p_H^s(R_5, R_7)$ can be written in the form

$$p_H^s(R_5, R_7) = p_H^e + (p_H^l - p_H^e) \frac{R_7(\tau)}{R_5(\tau) + R_7(\tau)}. \tag{5}$$

The constants p_H^e and p_H^l give the endosomal pH in early endosomes and late endosomes/lysosomes correspondingly.

One of the main ideas of our paper is the introduction of the stochastic variable T, which defines the point in time when the Rab conversion occurs. The time T can also be considered as the escape time of pH-sensitive nanoparticles and viruses from endosomes. We define it as the time when the values of Rab5 and Rab7 equalize as a result of rapid fall and rise, respectively. Observations from experiments show that noise has an impact on the variable T, leading to its alteration and consequently influencing the delayed or accelerated release of nanoparticles/viruses from endosomes.

The results of numerical simulations of stochastic differential Eq. (3) together with (4) and (5) by Wolfram Mathematics are illustrated in Figs. 2, 3, 4 and 5. Here, the dotted lines (panels (a)) designate the deterministic solution obtained from Eqs. (1) and (4). As this takes place, the stochastic trajectories of Rab5, Rab7 and pH are shown by the bundles of colored lines (panels (a)). The probability density functions (pdf) for T, Rab5, Rab7 and pH are illustrated by the histograms (panels (b), (c) and (d)), where the vertical dashed lines show the deterministic solutions for T (panels (b)), Rab5 (panels (c)) and Rab7 (panels (d)). The escape time of nanoparticles/viruses from endosomes shown by the horizontal dashed lines in Figs. 3a and 5a has been calculated by substituting T (the intersection point of Rab5 and Rab7 for deterministic solution, Fig. 1a) into $p_H(\tau)$ (Eq. (4), Fig. 1b) at $\tau = T = 880.044$ s. First, the noise-induced trajectories (colored bundles) in panels (a) pass in the vicinities of deterministic solutions (dotted lines). As this takes place, the width of bundles grows as noise increases (compare Figs. 2a and 4a for Rab5 and Rab7 as well as 3a and 5a for pH). As the noise intensity

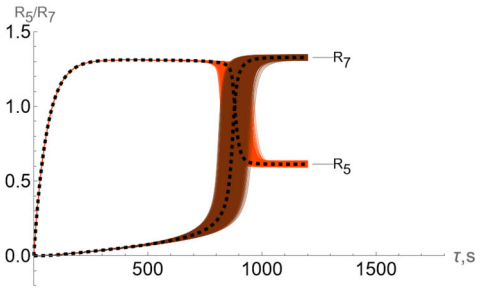

a Stochastic trajectories of Rab5 and Rab7 as the solutions of SDE (3).

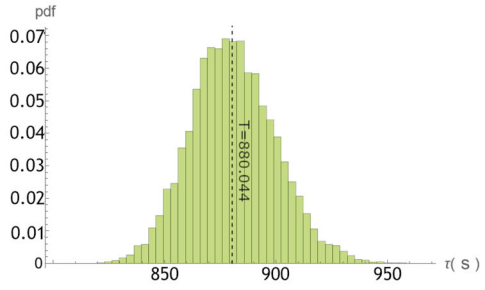

b Probability density function of the stochastic transition time T.

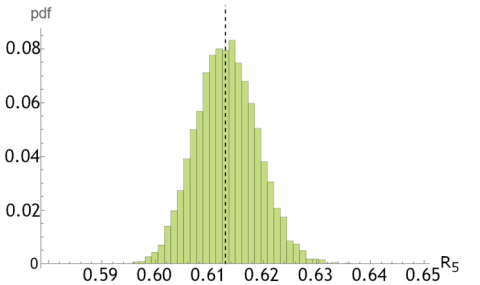

c Probability density function of Rab5 at time τ=1100 s.

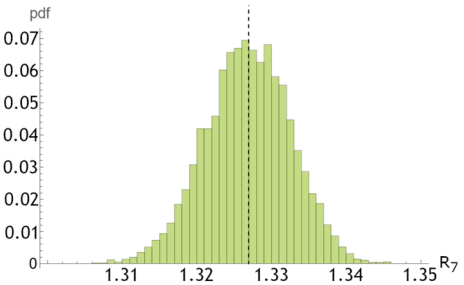

d Probability density function of Rab7 at time τ=1100 s.

Fig. 2 Numerical solution of the system (3) with the noise intensities $\sigma_5 = 0.2$, $\sigma_7 = 1.5$

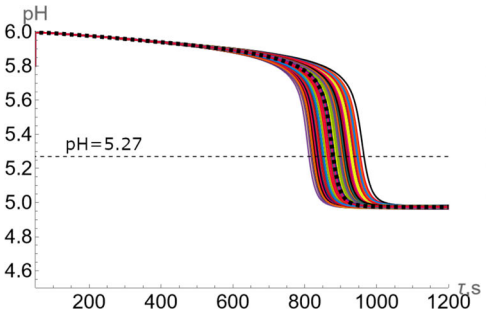

a Stochastic trajectories of pH as the solutions of equation (4).

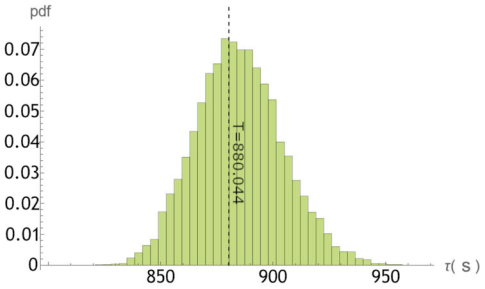

b Probability density function of $pH = 5.27$.

Fig. 3 Numerical solution of the system (3) with the noise intensities $\sigma_5 = 0.2$, $\sigma_7 = 1.5$

increases, the variable T shifts to the right or left of deterministic solution, resulting in a delayed or accelerated release of nanoparticles/viruses from endosomes, respectively. Namely, at low noise intensities σ_5 and σ_7 shown in Fig. 2b, we observe a nearly normal probability density function of the transition time T between 820 and 950 s. However, as the noise intensity increases, the range of time T expands (from 725 to 1100 s, Fig. 4b). As is easily seen from Fig. 4b, the pdf essentially differs from the normal distribution owing to lengthening of the right side of the histogram. In this case, the probability of large values of T increases leading to delayed release of nanoparticles/viruses from endosomes. In addition, the pdf peak shifts to the left as noise increases (compare Figs. 2b and 4b). Note that the dynamics of Rab5 and Rab7 are substantially different. Namely, when Rab5 and Rab7 fluctuate near the deterministic solutions at large times exceeding 1000 s in Figs. 2a and 4a, the upward Rab5 deviations become substantially larger than the corresponding downward deviations (compare the orange Rab5 bundles in Figs. 2a and 4a). This is accompanied by lengthening of the right side of Rab5 histogram (see Figs. 2c and 4c). As this takes place, the Rab7 pdf remains almost normal (see Figs. 2d and 4d). The nanoparticles/viruses release time from the endosomes was determined at $p_H = 5.27$ (see the horizontal lines in Figs. 3a and 5a) from the steady-state solution for $T = 880.044$ s. Our calculations show that the pH pdf tail lengthens to the right leading to a delayed nanoparticle/virus release time from the endosomes. As this takes place, the pdf peak shifts to the left as noise increases (compare Figs. 3b and 5b).

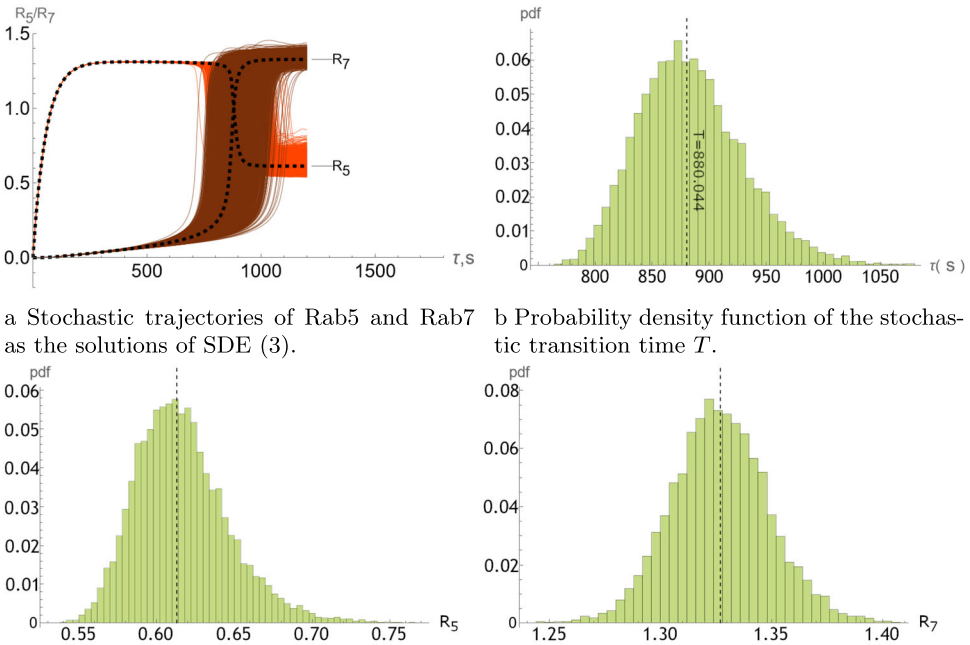

Fig. 4 Numerical solutions of SDE (3) with the intensities $\sigma_5 = 1$ and $\sigma_7 = 3.5$

a Stochastic trajectories of Rab5 and Rab7 as the solutions of SDE (3).

b Probability density function of the stochastic transition time T.

c Probability density function of Rab5 at time τ=1100 s.

d Probability density function of Rab7 at time τ=1100 s.

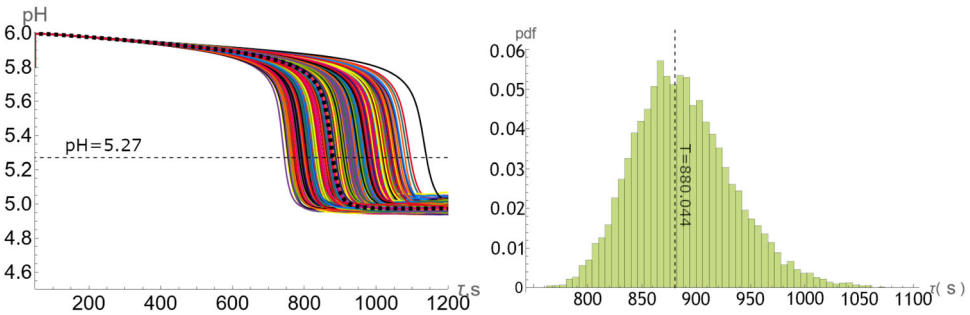

Fig. 5 Numerical solutions of SDE (3) with the intensities $\sigma_5 = 1$ and $\sigma_7 = 3.5$

a Stochastic trajectories of pH as the solutions of equation (4).

b Probability density function of $pH = 5.27$.

4 Summary and conclusions

We introduced a stochastic nonlinear model to describe the temporal dynamics of active Rab5 and Rab7 proteins on endosome surfaces and incorporated the endosomal acidification process. Using the nonlinear "cutoff switch" model for the conversion from Rab5 to Rab7, we added the multiplicative noises into the system and analyzed their impact on the random time T of Rab5 to Rab7 conversion. This time could also be interpreted as the escape time of pH-sensitive nanoparticles and viruses from endosomes. The probability density function for T was numerically analyzed. It shows that the average conversion time T is shifted to the right in comparison with the deterministic one. This shift affects both the pH distribution function and, consequently, the average escape time of viruses and nanoparticles from endosomes. Through numerical simulations of SDEs, we determined the probability density that characterizes the random fluctuations in endosomal pH. This could allow us to compute the probability of the endosomal pH falling below a critical threshold that gives the percentage of viruses and pH-responsive nanoparticles escaping endosomes. The introduction of multiplicative noises allows us to analyze the random escape time for nanoparticles/viruses leading to the conclusion that there is a higher likelihood of delaying nanoparticle release compared to accelerating it. Since the regulation of intracellular traffic is governed by the conversion from Rab5 to Rab7, it would be interesting to explore the connection of stochastic Rab5 to Rab7 conversion and stochastic anomalous intracellular transport of viruses and nanoparticles along microtubules to the perinuclear region [6, 7, 26, 27], fusion and fission inside cells [38–40].

Acknowledgements The research funding from the Ministry of Science and High Education of the Russian Federation (Ural Federal University Program of Development within the Priority-2030 Program) is gratefully acknowledged.

Data availability statement No data associated with the manuscript.

References

1. H. Hillaireau, P. Couvreur, Cell. Mol. Life Sci. **66**, 2873 (2009)
2. T.-G. Iversen, T. Skotland, K. Sandvig, Nano Today **6**, 176 (2011)
3. N.D. Donahue, H. Acar, S. Wilhelm, Adv. Drug Deliv. Rev. **143**, 68 (2019)
4. R. Augustine, A. Hasan, R. Primavera, R.J. Wilson, A.S. Thakor, B.D. Kevadiya, Mater. Today Commun. **25**, 101692 (2020)
5. M.S. de Almeida, E. Susnik, B. Drasler, P. Taladriz-Blanco, A. Petri-Fink, B. Rothen-Rutishauser, Chem. Soc. Rev. **50**, 5397 (2021)
6. P.C. Bressloff, J.M. Newby, Rev. Mod. Phys. **85**, 135 (2013)
7. S. Fedotov, N. Korabel, T.A. Waigh, D. Han, V.J. Allan, Phys. Rev. E **98**, 042136 (2018)
8. T. Lagache, O. Danos, D. Holcman, Biophys. J . **102**, 980 (2012)
9. J.M. White, G.R. Whittaker, Traffic **17**, 593 (2016)
10. T. Lagache, C. Sieben, T. Meyer, A. Herrmann, D. Holcman, Front. Phys. **5**, 25 (2017)
11. J. Rink, E. Ghigo, Y. Kalaidzidis, M. Zerial, Cell **122**, 735 (2005)
12. D. Poteryaev, S. Datta, K. Ackema, M. Zerial, A. Spang, Cell **141**, 497 (2010)
13. L.I. Selby, C.M. Cortez-Jugo, G.K. Such, A.P. Johnston, Wiley Interdiscip. Rev. Nanomed. Nanobiotechnol. **9**, e1452 (2017)
14. N. Kongkatigumjorn, S.A. Smith, M. Chen, K. Fang, S. Yang, E.R. Gillies, A.P. Johnston, G.K. Such, A.C.S. Appl, Nano Mater. **1**, 3164 (2018)
15. N. Deirram, C. Zhang, S.S. Kermaniyan, A.P. Johnston, G.K. Such, Macromol. Rapid Commun. **40**, 1800917 (2019)
16. T. Andrian, R. Riera, S. Pujals, L. Albertazzi, Nanoscale Adv. **3**, 10 (2021)
17. K. Zhou, Y. Wang, X. Huang, K. Luby-Phelps, B.D. Sumer, J. Gao, Angew. Chem. Int. Ed. **50**, 6109 (2011)
18. P. del Conte-Zerial, L. Brusch, J.C. Rink, C. Collinet, Y. Kalaidzidis, M. Zerial, Deutsch. Mol. Syst. Biol. **4**, 206 (2008)
19. M. Castro, G. Lythe, J. Smit, C. Molina-París, Sci. Rep. **11**, 7845 (2021)
20. S. Fedotov, D. Alexandrov, I. Starodumov, N. Korabel, Mathematics **10**, 375 (2022)
21. V. Sholokhov, E.V. Makoveeva, S. Fedotov, I.O. Starodumov, D.V. Alexandrov, Eur. Phys. J. Special Top. **232**, 1219 (2023)
22. J. Rink, E. Ghigo, Y. Kalaidzidis, M. Zerial, Cell **122**, 735 (2005)
23. H.M. Van Der Schaar, M.J. Rust, C. Chen, H. Van Der Ende-Metselaar, J. Wilschut, X. Zhuang, J.M. Smit, PLoS Pathog. **4**, e1000244 (2008)
24. D.V. Alexandrov, I.A. Bashkirtseva, M. Crucifix, L.B. Ryashko, Phys. Rep. **902**, 1 (2021)
25. D.V. Alexandrov, I.A. Bashkirtseva, L.B. Ryashko, Phys. D **343**, 28 (2017)
26. N. Korabel, D. Han, A. Taloni, G. Pagnini, S. Fedotov, V. Allan, T.A. Waigh, Entropy **23**, 958 (2021)
27. D. Han, D.V. Alexandrov, A. Gavrilova, S. Fedotov, Fractal Fract. **5**, 221 (2021)
28. C. Simpson, Y. Yamauchi, Viruses **12**, 117 (2020)
29. S. Wannasarit, S. Wang, P. Figueiredo, C. Trujillo, F. Eburnea, L. Simón-Gracia, A. Correia, Y. Ding, T. Teesalu, D. Liu et al., Adv. Funct. Mater. **29**, 1905352 (2019)
30. C.B. Braga, L.A. Kido, E.N. Lima, C.A. Lamas, V.H. Cagnon, C. Ornelas, R.A. Pilli, A.C.S. Biomater, Sci. Eng. **6**, 2929 (2020)
31. S.M. Figueroa, D. Fleischmann, A. Goepferich, J. Control. Release **329**, 552 (2021)
32. X.Y. Ma, B.D. Hill, T. Hoang, F. Wen, Semin. Cancer Biol. **86**, 1143 (2022)
33. M. Maugeri, M. Nawaz, A. Papadimitriou, A. Angerfors, A. Camponeschi, M. Na et al., Nat. Commun. **10**(1), 4333 (2019)
34. K. Koitabashi, H. Nagumo, M. Nakao, T. Machida, K. Yoshida, K. Sakai-Kato, Biochim. Biophys. Acta (BBA)-Biomembranes **1863**(8), 183627 (2021)
35. P. Paramasivam, C. Franke, M. Stöter, A. Höijer, S. Bartesaghi, A. Sabirsh et al., J. Cell Biol. **221**(2), e202110137 (2021)
36. M. Herrera, J. Kim, Y. Eygeris, A. Jozic, G. Sahay, Biomater. Sci. **9**, 4289 (2021)

37. A. Spadea, M. Jackman, L. Cui, S. Pereira, M.J. Lawrence, R.A. Campbell, M. Ashford, A.C.S. Appl, Mater. Interfaces **14**(26), 30371 (2022)
38. L. Foret, J.E. Dawson, R. Villaseñor, C. Collinet, A. Deutsch, L. Brusch, M. Zerial, Y. Kalaidzidis, F. Jülicher, Curr. Biol. **22**, 1381 (2012)
39. D.V. Alexandrov, N. Korabel, F. Currell, S. Fedotov, Cancer Nanotech. **13**, 15 (2022)
40. E.V. Makoveeva, D.V. Alexandrov, S.P. Fedotov, Crystals **12**, 1159 (2022)